

# Entanglement distribution in pure-state quantum networks

Sébastien Perseguers\* and J. Ignacio Cirac

*Max-Planck-Institut für Quantenoptik, Hans-Kopfermann-Strasse 1, D-85748 Garching, Germany*Antonio Acín<sup>1,2</sup> and Maciej Lewenstein<sup>1,2</sup><sup>1</sup>*ICFO-Institut de Ciències Fotòniques, Mediterranean Technology Park, E-08860 Castelldefels (Barcelona), Spain*<sup>2</sup>*ICREA-Institució Catalana de Recerca i Estudis Avançats, Lluís Companys 23, 08010 Barcelona, Spain*

Jan Wehr

*Department of Mathematics, The University of Arizona, Tucson, Arizona 85721-0089, USA*

(Received 6 November 2007; published 7 February 2008)

We investigate entanglement distribution in pure-state quantum networks. We consider the case when non-maximally entangled two-qubit pure states are shared by neighboring nodes of the network. For a given pair of nodes, we investigate how to generate the maximal entanglement between them by performing local measurements, assisted by classical communication, on the other nodes. We find optimal measurement protocols for both small and large one-dimensional networks. Quite surprisingly, we prove that Bell measurements are not always the optimal ones to perform in such networks. We generalize then the results to simple small two-dimensional (2D) networks, finding again counterintuitive optimal measurement strategies. Finally, we consider large networks with hierarchical lattice geometries and 2D networks. We prove that perfect entanglement can be established on large distances with probability one in a finite number of steps, provided the initial entanglement shared by neighboring nodes is large enough. We discuss also various protocols of entanglement distribution in 2D networks employing classical and quantum percolation strategies.

DOI: [10.1103/PhysRevA.77.022308](https://doi.org/10.1103/PhysRevA.77.022308)

PACS number(s): 03.67.Mn

## I. INTRODUCTION

Quantum networks [1,2] play a key role in quantum-information processing. In such networks, quantum states can be prepared initially and shared between neighboring nodes (or stations), i.e., entanglement can be generated, and this resource is then to be used for quantum communication [3,4], or distributed quantum computation [5] involving arbitrary nodes of the network. One of the main tasks is then to design protocols that use the available quantum correlations to entangle two distant nodes of the network, and to optimize these protocols in terms of final entanglement and probability of success.

A set of quantum repeater stations, for instance [see Fig. 1(a)], can be considered as a one-dimensional (1D) quantum network, where the aim is to establish quantum communication over large distances [6–9]. It is well known that the simple entanglement swapping [10] procedure can achieve this goal. Entanglement swapping [see Fig. 1(b)] consists in performing a joint Bell measurement, i.e., a measurement in an orthonormal basis of maximally entangled states at the nodes *B* and *C*, in order to achieve the entanglement between the nodes *A* and *D*. This protocol is then repeated between the further nodes of the network [see Fig. 1(c)]. Unfortunately, except for the unrealistic case of perfect resources and operations, the probability of obtaining entanglement between the end nodes of such a network decays exponentially with the number of repeaters. This problem can be overcome by the more sophisticated quantum repeaters protocols [6–9]

which intersperse connection steps (entanglement swapping) with purification and distillation steps and result only in a polynomial decay, thus opening the way for feasible long-distance quantum communication. This way is not free of obstacles, however. In particular, its technical realization requires the development of efficient and reliable quantum memories [9,11].

In a recent work [12], we have proposed an approach which can be regarded as an alternative to the repeaters method and which exploits the high connectivity of the quantum network. In particular, in two-dimensional or higher dimensional lattices of arbitrarily large size, a perfect connection between any two nodes is possible with a probability that is strictly greater than zero, even with imperfect resources. This can be achieved by the so-called entanglement percolation strategies, which will be discussed in the next sections. The inspiration used in the construction of these strategies comes from classical bond percolation theory. Classical bond percolation describes many phenomena that we know from everyday life, from fluid dynamics in porous media to propagation of forest fires [13,14]. An introduction to this concept is given in Appendix A, where we collect the

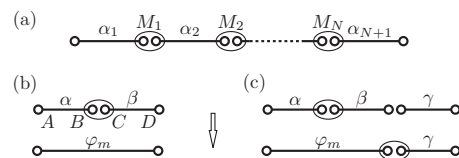


FIG. 1. Notation and examples of 1D networks: (a) the standard quantum repeater scenario; (b) entanglement swapping; (c) a two-repeater system.

\*sebastien.perseguers@mpq.mpg.de

main ideas from classical percolation used in the present study. In the context of quantum networks, by entanglement percolation strategies we mean any protocol consisting of local operations and classical communication (LOCC) such that two distant nodes in an arbitrarily large lattice share an entangled state.

The fact that percolation strategies work is in itself very encouraging, but it remains of little use for finite and small networks [15,16]. The aim of the present paper is twofold: first, we investigate and derive optimal local measurement protocols for simple networks of finite size. In particular, we consider certain 1D and two-dimensional (2D) networks of nodes that consist of  $z$  qubits, where  $z$  is the number of neighbors. Neighboring nodes share *partially* entangled pure states. We apply then local quantum operations to the nodes, assuming that these operations are noiseless. We first address the question of optimal entanglement propagation in small networks consisting of three or four nodes only. The insights obtained for these simple situations are then used as building blocks for larger 1D and 2D quantum networks, as well as networks with hierarchical geometry.

Our second aim is to discuss examples of hierarchical “diamond” and “tree” lattices, in which perfect entanglement on arbitrarily large distances can be achieved in a finite number of steps (measurements). Provided that sufficiently large, but not necessarily maximal entanglement is present, we can convert connections along a given line into perfect singlets. Finally, we consider various kinds of percolation strategies: the one presented in Ref. [12], which employs a change in the lattice connectivity due to quantum measurements, and a different one in a triangular lattice, where the optimal singlet conversion strategy is used. Both of these protocols essentially demonstrate that the quantum percolation thresholds are lower than their classical counterparts. Equally interesting we propose to use the optimal singlet conversion strategy to transform a square lattice into two independent square lattices of doubled size, for which the percolation probability is larger than in the original lattice.

*Outline.* In Sec. II we fix the notation and define the figures of merit used for evaluating the measurements efficiency: the concurrence ( $C$ ), the so-called worst case entanglement (WCE) and the singlet conversion probability (SCP). In Sec. III we describe the strategies maximizing these quantities for some 1D networks, starting from a simple one-repeater configuration, consisting of two bonds with two imperfectly entangled pairs on them. Interestingly, there exists a strategy that conserves the averaged singlet conversion probability [17]; the protocol, however, does not scale with the number of repeaters, as expected. Section III B deals with the problem of two repeaters, that is, three bonds. Here the optimization of the SCP is much more complex: in some conditions we obtain that the optimal measurements do not correspond to a Bell measurement. This result is somewhat analogous to the recent result by Modławska and Grudka [18], who have demonstrated that nonmaximally entangled states can be better for the realization of multiple linear optical teleportation in the scheme of Knill, Laflamme, and Milburn [19]. The last part of this section deals with a large 1D network (i.e., in the limit of infinite size network). Here we prove that the probability of establishing entangle-

ment over large distances decays exponentially. We present optimal strategies for the concurrence and the WCE, and upper bounds for the SCP.

In Sec. IV we turn to the simplest small network in 2D: a square. We obtain similar results as in the case of two repeaters in 1D, indicating that Bell measurements do not always provide the best protocol. In Section V we apply the results of previous sections to networks of large size and hierarchical geometry, that is, lattices that iterate certain geometric structures, so that at each level of iterations the number of nodes, or the number of neighbors changes. We consider two kinds of hierarchical lattices: first we discuss the so-called “diamond” lattice, for which we prove that for sufficiently large initial entanglement, one can establish perfect entanglement on large scales (i.e., some lower levels of iteration) in a finite number of steps. A somewhat simpler result holds for the simplest possible double Cayley tree lattice, in which in each step of iteration each bond branches into two. For such lattices, if the initial entanglement is large enough, perfect entanglement can be established at each level of iteration.

Finally, in Sec. VI we consider genuine 2D lattices. First, using a similar method as in Sec. V we show that for a sufficiently broad strip of a square lattice, we can convert connections of a given line along the strip into a line of perfect singlets, provided, of course, that initially an imperfect, but sufficiently large entanglement is present. Second we reconsider percolation strategies in the limit of large lattices and discuss the example of hexagonal lattice with double bonds from Ref. [12], and a triangular lattice with variable bonds. In the first of these examples quantum measurements lead to local reduction of the SCP, but change the geometry of the lattice, increasing its connectivity and thus the classical percolation threshold. In the second example we use a protocol optimizing the SCP to transform the original lattice to a new one with the same geometry, but with a higher probability  $p$  of getting a singlet on a bond. Similarly, we discuss a different type of strategy, where by using the optimal singlet conversion protocol we transform a square lattice into two independent square lattices with the same mean SCP as the initial one. We prove that the classical probability of connecting a pair of neighboring points in the initial lattice (two neighboring points from the two lattices) to another such pair is strictly larger for the case of two lattices. We conclude then in Sec. VII.

## II. PRELIMINARIES: NOTATION AND BASIC NOTIONS

Throughout this work, a pure state of two qubits is represented by a solid line in the figures and is written (except when specified) as

$$|\alpha\rangle = \sqrt{\alpha_0}|00\rangle + \sqrt{\alpha_1}|11\rangle, \quad (1)$$

where  $\alpha_0 + \alpha_1 = 1$  and  $\alpha_0 \geq \alpha_1$  (it is assumed that local basis rotations are performed whenever necessary for the states to be written in that way). This defines the Schmidt decomposition of a pure state of two qubits, while  $\alpha_0$  and  $\alpha_1$  are their Schmidt coefficients.

A general measurement, also known as positive operator valued measure (POVM), is described by  $n$  positive opera-

tors  $E_m \in M_4(\mathbb{C})$  satisfying the completeness relation  $\sum_{m=1}^n E_m = \mathbb{1}_4$ . Consider a one-repeater configuration such as in Fig. 1(b) where the connecting states are  $|\alpha\rangle$  and  $|\beta\rangle$  and a measurement  $M$  is applied at the repeater. Let

$$\rho_m = \text{tr}_B[(\mathbb{1}_2 \otimes E_m \otimes \mathbb{1}_2)|\alpha\beta\rangle\langle\alpha\beta|]$$

be the resulting non-normalized state of the measurement  $M$ , which occurs with a probability  $p_m = \text{tr}(\rho_m)$ . We consider in this paper projective measurements only, i.e.,  $n=4$  and  $E_m = |u_m\rangle\langle u_m|$  for some normalized state  $|u_m\rangle$ . For such measurements the smallest Schmidt coefficient of  $\rho_m$  is  $\lambda_m = \min\{\text{eig}(\tilde{\rho}_m)\}/p_m$ , where  $\tilde{\rho}_m = \text{tr}_A(\rho_m)$ , or equivalently

$$\lambda_m = \frac{1}{2} \left( 1 - \sqrt{1 - \frac{4 \det(\tilde{\rho}_m)}{p_m^2}} \right). \quad (2)$$

Considering the following map from  $\mathbb{C}^2 \otimes \mathbb{C}^2$  to  $M(\mathbb{C}, 2)$ :

$$|a\rangle = \sum_{i,j=0}^1 a_{ij}|ij\rangle \mapsto \hat{a} = \begin{pmatrix} a_{00} & a_{01} \\ a_{10} & a_{11} \end{pmatrix}, \quad (3)$$

one can show that  $\tilde{\rho}_m$  is now equal to  $X_m X_m^\dagger$ , with  $X_m = \hat{a} \hat{u}_m \hat{\beta}$ .

The concurrence of a state  $\varphi$  is by definition  $C(\varphi) \equiv 2|\det(\hat{\varphi})|$ . Therefore, the concurrence  $C_m$ , the smallest Schmidt coefficient  $\lambda_m$ , and the outcome probability  $p_m$  are explicitly given by

$$C_m = \frac{2|\det(X_m)|}{p_m} = \frac{\sqrt{\alpha_0 \alpha_1 \beta_0 \beta_1}}{p_m} C(u_m), \quad (4a)$$

$$\lambda_m = \frac{1}{2} (1 - \sqrt{1 - C_m^2}), \quad (4b)$$

$$p_m = \sum_{i,j=0}^1 \alpha_i \beta_j |\hat{u}_{m,ij}|^2. \quad (4c)$$

### 1. Entanglement swapping

A basic operation for propagating entanglement over larger distances is the so-called ‘‘entanglement swapping’’ [see Fig. 1(b)]. It corresponds to the case in which a Bell measurement is performed at the repeaters. A Bell measurement is nothing but a measurement in the Bell basis, introduced in what follows.

Starting from the computational basis  $\{|0\rangle, |1\rangle\}$  of a single qubit, we define the new basis  $\{|\uparrow\rangle, |\downarrow\rangle\}$ ,

$$\begin{pmatrix} |\uparrow\rangle \\ |\downarrow\rangle \end{pmatrix} = U \begin{pmatrix} |0\rangle \\ |1\rangle \end{pmatrix}, \quad U \in \mathcal{U}(2), \quad (5)$$

and the Bell vectors

$$|\Phi^\pm\rangle = \frac{|\uparrow\uparrow\rangle \pm |\downarrow\downarrow\rangle}{\sqrt{2}} \quad \text{and} \quad |\Psi^\pm\rangle = \frac{|\uparrow\downarrow\rangle \pm |\downarrow\uparrow\rangle}{\sqrt{2}}, \quad (6)$$

which give a basis in  $\mathbb{C}^2 \otimes \mathbb{C}^2$ . Two specific bases play a key role in this paper: the computational or ZZ basis, where the

vectors  $|\uparrow\rangle$  and  $|\downarrow\rangle$  for both qubits are the eigenvectors of the Pauli matrix  $\sigma_z$ , and the XZ basis, where the first basis is chosen as being the eigenvectors of  $\sigma_x$ . Although we could, in principle, parametrize the Bell states in that way, calculations are much easier and clearer in the ‘‘magic basis’’ defined as [20]

$$(\hat{\Phi}_1, \hat{\Phi}_2, \hat{\Phi}_3, \hat{\Phi}_4) = (\mathbb{1}_2, -i\sigma_z, i\sigma_y, -i\sigma_x)|\Phi^+\rangle. \quad (7)$$

In this basis, the concurrence of a state  $|\mu\rangle = \sum_{i=1}^4 \mu_i |\Phi_i\rangle$  simply reads  $C(\mu) = |\sum_{i=1}^4 \mu_i|^2$ . It follows that the coefficients  $\mu_i$  of a Bell state (whose concurrence is 1 by definition) have all the same phase; hence we can choose them as being real. Let a set of four such states  $\{\mu_m\}$ , so that the matrix  $(\mu_{m,i})$  belongs to  $\mathcal{SO}(4)$ . Then the probabilities given in Eq. (4c) read

$$p_m = p_{\min}(\mu_{m,1}^2 + \mu_{m,2}^2) + p_{\max}(\mu_{m,3}^2 + \mu_{m,4}^2), \quad (8)$$

with

$$p_{\min} = \frac{\alpha_0 \beta_1 + \alpha_1 \beta_0}{2} \quad \text{and} \quad p_{\max} = \frac{\alpha_0 \beta_0 + \alpha_1 \beta_1}{2}. \quad (9)$$

We emphasize the fact that (given two states  $\alpha$  and  $\beta$ ), the outcome probabilities completely characterize a Bell measurement, since  $\lambda_m$  depends only on  $p_m$  for  $C(u_m) = 1$  [see Eq. (4)].

### 2. Figures of merit

We describe here three figures of merit used to evaluate the usefulness of an entanglement distribution protocol: the concurrence, the singlet conversion probability (SCP), and the worst-case entanglement (WCE). All these figures of merit take value in the interval  $[0, 1]$ .

*Concurrence.* The average concurrence of a measurement  $M$  is defined as

$$C_M = \sum_m p_m C_m, \quad (10)$$

where  $C_m$  is the concurrence of the outcome  $m$  and  $p_m$  is the corresponding probability.

*WCE.* The idea of the WCE is to find a measurement optimizing the entanglement for all its outcomes. Taking the smallest Schmidt coefficient as the entanglement measure we define the WCE as

$$W_M = 2 \min_m \{\lambda_m\}. \quad (11)$$

*SCP.* We consider here the probability of conversion of a given state into a perfect singlet. A result from majorization theory [21, 22] tells us that a state  $|\alpha\rangle$  can be converted into a singlet by LOCC with maximal probability  $2\alpha_1$  through the ‘‘Procrustean method’’ of entanglement concentration described in [23]. More in general, the LOCC conversion between entangled pure states of two parties is governed by majorization theory, as follows from the works by Nielsen and Vidal [21, 24]. Throughout this work, several results from majorization theory on LOCC transformations between entangled states are used. A short introduction to this topic is given in Appendix B; more details can be found in Ref. [22].

We define the average SCP for a measurement  $M$  as

$$S_M = 2 \sum_m p_m \lambda_m, \quad (12)$$

where  $\lambda_m$  is the smallest Schmidt coefficient of the outcome  $m$ . Since this figure of merit is used for different systems, we sometimes use the following notation for clarity:

$$S_M^{(N)}(\alpha_{1,0}, \alpha_{2,0}, \dots, \alpha_{N+1,0}),$$

where  $N$  means the number of repeaters of a 1D chain consisting of  $N+1$  states  $\alpha_1, \alpha_2, \dots, \alpha_{N+1}$ , as depicted in Fig. 1(a).

### III. 1D NETWORKS

Before studying complex networks, it is worth looking at systems made of one or two repeaters only. In fact, some interesting properties of these small systems can then be used in more elaborated strategies for larger networks. For instance, the important fact that the SCP does not decrease after one measurement (Sec. III A 3) allows one to get better results for the percolation on honeycomb lattices [12]. Another important and surprising result is that Bell measurements are not, in general, the measurements that maximize the SCP (Sec. III B 2), although they are the best ones for the average concurrence and the WCE. Previous results on 1D networks can also be found in Refs. [17,25,26].

#### A. One repeater

We consider in this section a system consisting of two states  $\alpha$  and  $\beta$  joined by a single repeater [see Fig. 1(b)]. We first prove a general statement on Bell measurements, and then describe the measurements that maximize our three figures of merit.

##### 1. Bell measurements and outcome probabilities

The following result is very useful when trying to maximize the SCP over the set of Bell measurements (the proof is given in Appendix C).

*Result 1.* Outcome probabilities for a one-repeater Bell measurement. Let  $\{x_m\}$  be four real numbers that add up to one and that lie in the interval  $[p_{\min}, p_{\max}]$ . Then there exists a Bell measurement whose outcome probabilities  $p_m$  are equal to  $x_m$ .

##### 2. Maximizing the concurrence and the WCE

It is clear from Eqs. (4a) and (10) that any Bell measurement, i.e.,  $C(u_m) = 1 \forall m$ , maximizes the average concurrence, and therefore

$$C_{\max} = 2\sqrt{\alpha_0 \alpha_1 \beta_0 \beta_1}. \quad (13)$$

The result of the maximization of the WCE is summarized in the following result.

*Result 2.* Best WCE strategy for one repeater. The maximum value of  $W$  for a one-repeater system is reached by the Bell measurement in the XZ basis, with

$$W_{\max} = W_{XZ} = 1 - \sqrt{1 - 16\alpha_0 \alpha_1 \beta_0 \beta_1}. \quad (14)$$

*Proof (by contradiction).* The Bell states  $|u_m\rangle$  in the XZ basis are given by the columns of the matrix

$$M_{XZ} = \frac{1}{2} \begin{pmatrix} -1 & 1 & 1 & 1 \\ 1 & -1 & 1 & 1 \\ 1 & 1 & -1 & 1 \\ 1 & 1 & 1 & -1 \end{pmatrix},$$

hence  $p_m = 1/4$  and  $2\lambda_m = 1 - \sqrt{1 - 16\alpha_0 \alpha_1 \beta_0 \beta_1} \forall m$ . Now suppose that there exists a measurement  $M$  described by the set  $\{E_m = |u_m\rangle\langle u_m|\}_{m=1}^n$ , with  $n \geq 4$ , such that  $W_M > W_{XZ}$ . Then each  $\lambda_m$  has to be strictly greater than the smallest Schmidt coefficient of the outcomes in the XZ basis. Thus, from Eq. (2)

$$\det(\tilde{\rho}_m) > p_m^2 4\alpha_0 \alpha_1 \beta_0 \beta_1 \quad \forall m. \quad (15)$$

Since  $\det(\tilde{\rho}_m) = \alpha_0 \alpha_1 \beta_0 \beta_1 |\det(\hat{u}_m)|^2$ , the summation over  $m$  of the square root of Eq. (15) yields

$$\sum_{m=1}^n |\det(\hat{u}_m)| > 2. \quad (16)$$

But the concurrence of a (normalized) state is smaller than or equal to 1, hence  $2|\det(\hat{u}_m)| \leq \|u_m\|^2$ . Moreover, taking the trace of the completeness relation for the operators  $E_m$  implies  $\sum_{m=1}^n \|u_m\|^2 = 4$ . Therefore  $\sum_{m=1}^n |\det(\hat{u}_m)| \leq 2$ , which is in contradiction with Eq. (16), and concludes the proof. ■

#### 3. Maximizing the SCP

The following result gives the maximum value of the SCP for one entanglement swapping step.

*Result 3.* Best SCP strategy for one repeater. The measurement that maximizes  $S$  for a one-repeater configuration is the Bell measurement in the ZZ basis, and

$$S_{\max} = S_{ZZ} = 2 \min\{\alpha_1, \beta_1\}. \quad (17)$$

*Proof.* Two kinds of outcomes appear when performing a Bell measurement in the computational basis: two of the outcome probabilities are equal to  $p_{\max}$ , while the other two are equal to  $p_{\min}$ . Putting these values into Eq. (4) one finds the corresponding smallest Schmidt coefficients as follows:

$$\lambda(p_{\max}) = \frac{\alpha_1 \beta_1}{2p_{\max}}, \quad \lambda(p_{\min}) = \frac{\min\{\alpha_0 \beta_1, \alpha_1 \beta_0\}}{2p_{\min}}, \quad (18)$$

whence  $S_{ZZ} = 2 \min\{\alpha_1, \beta_1\}$ . Consider now that we are allowed to perform some arbitrary unitary not only on  $BC$ , but on  $ABC$ . We are in the presence of a bipartite system, and the results of majorization theory apply: the SCP of this system is at most  $2\beta_1$ . A similar construction for qubits  $B$ ,  $C$ , and  $D$  tells us that the SCP is at most  $2\alpha_1$ , so that the final SCP cannot exceed twice the minimum of  $\alpha_1$  and  $\beta_1$ . ■

*Remark.* Setting  $\alpha = \beta$ , one sees that the SCP does not decrease after one entanglement swapping; this is the ‘‘conserved entanglement’’ described in [17].

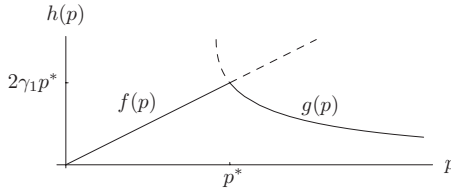


FIG. 2. Representation of the function  $h(p)=\min\{f(p),g(p)\}$  governing the SCP after Bell measurements in a two-repeater configuration.

## B. Two repeaters

We consider a system of three states on which we perform two consecutive measurements, as shown in Fig. 1(c), and we describe those measurements that maximize the three figures of merit.

### 1. Maximizing the concurrence and the WCE

The maximization of these two figures of merit is trivial for a two-repeater configuration once one knows the results for the one-repeater system. First, any Bell measurement maximizes the average concurrence of the results of the two measurements. This will be generalized and proved for any number of repeaters in Sec. III C 1. Then, in order to maximize the WCE, we simply have to perform XZ measurements at both repeaters. In fact, if we perform any other measurement on the first repeater, then at least one resulting state  $\varphi_m$  will be less entangled than the XZ results, and this reflects on the WCE of the second measurement (which has to be a Bell measurement in the XZ basis from Result 2).

### 2. Maximizing the SCP

After the first measurement, we get four resulting states  $|\varphi_m\rangle$  with probabilities  $p_m$ . From Result 3 we know that for any outcome, the second measurement has to be done in the ZZ basis. Hence, we have to find the first measurement  $M$  that maximizes

$$S_M^{(2)}(\alpha_0, \beta_0, \gamma_0) = 2 \sum_m p_m \min\{\varphi_{m,1}, \gamma_1\}. \quad (19)$$

We first maximize this quantity over the set of Bell measurements (which, as we will see, leads to the best strategy for a large range of entangled states  $\alpha$ ,  $\beta$ , and  $\gamma$ ), and then we present some numerical results showing that non-Bell measurements sometimes provide better results.

*Bell measurements.* We fix the states  $\alpha$ ,  $\beta$ , and  $\gamma$  and we consider the SCP as a function of the outcome probabilities only.

$$S(\{p_m\}) = \sum_m \min\{f(p_m), g(p_m)\} \equiv \sum_m h(p_m), \quad (20)$$

where  $f(p)=2\gamma_1 p$  and  $g(p)=p-\sqrt{p^2-\alpha_0\alpha_1\beta_0\beta_1}$ . One can show that  $g'(p)<0$  and  $g''(p)>0 \forall p \in [p_{\min}, p_{\max}]$ . A typical plot of  $h(p)$  is shown in Fig. 2, and the value  $p^*$  at which the functions  $f$  and  $g$  cross each other is

$$p^* = \frac{1}{2} \sqrt{\frac{\alpha_0\alpha_1\beta_0\beta_1}{\gamma_0\gamma_1}}. \quad (21)$$

TABLE I. Maximization of  $S^{(2)}$  over Bell measurements (see the text for details).

Value of $p^*$	$\{p_m\}$ maximizing $S^{(2)}$
$p^* \leq p_{\min}$	$\{p_{\min}, p_{\min}, p_{\max}, p_{\max}\}$
$p_{\min} \leq p^* \leq (1-p_{\max})/3$	$\{p^*, p^*, p_{\max}, 1-2p^*-p_{\max}\}$
$(1-p_{\max})/3 \leq p^* \leq 1/4$	$\{p^*, p^*, p^*, 1-3p^*\}$
$p^* \geq 1/4$	$\{1/4, 1/4, 1/4, 1/4\}$

It is sufficient to maximize the function over the possible probability distributions, since Result 1 insures the existence of a Bell measurement leading to this optimal distribution; we recall that the probabilities have to be chosen in the interval  $[p_{\min}, p_{\max}]$ . Let us give two necessary conditions that have to be satisfied by the best probability distribution (they can be proven rigorously, but a look at Fig. 2 may be clearer):

(a) If the set  $\{p_m\}$  maximizes  $S$ , then all probabilities lie either to the left of  $p^*$  or to its right. In fact, suppose, for example, that  $p_1+2\varepsilon < p^* < p_2-2\varepsilon$ , and choose  $\tilde{p}_1=p_1+\varepsilon$  and  $\tilde{p}_2=p_2-\varepsilon$  (with  $0 < \varepsilon \leq 1$  as it should be). The constraints on these new probabilities are clearly satisfied if it was the case before, and a better SCP has been found.

(b) If  $p_1$  and  $p_2$  are such that  $p^*+2\varepsilon < p_1 \leq p_2 < p_{\max}-2\varepsilon$ , then the choice  $\tilde{p}_1=p_1-\varepsilon$  and  $\tilde{p}_2=p_2+\varepsilon$  gives rise to a strictly greater SCP (this comes from the convexity of  $g$ ).

It is now simple to maximize the SCP of two repeaters, and one sees that the value  $p^*$ , with respect to  $p_{\min}$  and  $p_{\max}$ , plays a crucial role in the choice of the best probability distribution. In fact, we have to distinguish four distinct cases (see the results in Table I). We notice that ZZ measurements lead to the maximum SCP whenever  $p^* \leq p_{\min}$ , while the XZ ones are the best strategy for  $p^* \geq 1/4$ . So far, we have maximized the SCP for two repeaters supposing that the first measurement was to be done on the states  $\alpha$  and  $\beta$ . But what happens if we start from the right side? It appears that the maximum SCP depends, in general, on the order of the measurements and that performing the first measurement where the states are more entangled yields better results.

*General measurements (numerical results).* The question is to check if some non-Bell measurements yield a better SCP than the results of the last paragraph. Since the concurrence of the states used for entanglement swapping can now take any value between 0 and 1, we cannot consider  $S$  as a function of the outcome probabilities only. But for a fixed concurrence  $C < 1$  one sees that

$$\bar{g}(C, p) \equiv p - \sqrt{p^2 - \alpha_0\alpha_1\beta_0\beta_1 C^2} < g(p) \quad \forall p.$$

Writing the corresponding variables of non-Bell measurements with a bar, we have that  $\bar{p}^* < p^*$  and  $\bar{g}(C, \bar{p}^*) < g(p^*)$ . Therefore, one can check that Bell measurements are indeed the best ones, except, possibly, when  $p_{\min} \leq p^* \leq (1-p_{\max})/3$ . The key fact about Bell measurements in that case is that we cannot choose three outcome probabilities to lie on  $p^*$ , since the fourth one would be greater than  $p_{\max}$ . But the range of possible outcome probabilities depends on

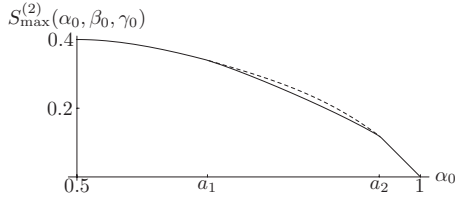


FIG. 3. SCP for a system of two repeaters, with  $\beta_0 = \gamma_0 = 0.7$ . Numerical results (dashed line) show that there exists a better strategy than Bell measurements (solid line) for  $\alpha_0 \in [a_1, a_2]$ . The values  $a_1$  and  $a_2$  are such that  $p^*(a_1) = [1 - p_{\max}(a_1)]/3$  and  $p^*(a_2) = p_{\min}(a_2)$ .

the concurrence: for example, from Eq. (4c) and for  $C(u_m) = 0$ , we have that  $\bar{p}_m \in [\alpha_1 \beta_1, \alpha_0 \beta_0]$ , or more generally,

$$\bar{p}_m \in [\bar{p}_{\max}, \bar{p}_{\min}] \supseteq [p_{\max}, p_{\min}]. \quad (22)$$

Hence, and this is confirmed by numerical results, a better strategy is to perform a measurement such that three outcomes probabilities are equal to  $\bar{p}^*$ , and that the concurrences of the states are the largest ones satisfying  $\bar{p}_{\max} = 1 - 3\bar{p}^*$ . Our numerical evidence shows that Bell measurements do not always maximize the SCP (see Fig. 3).

### C. Large 1D chains

We consider the system of Fig. 1(a) that consists of  $N$  repeaters joining  $N+1$  states. For simplicity, we choose the states  $\alpha_i$  as being identical:  $|\alpha_i\rangle = |\varphi\rangle \forall i$ . We show in this section which strategies yield the optimal solution for the concurrence and the WCE, and for the SCP we give an upper bound to its maximum value and some results for XZ and ZZ measurements.

#### 1. Maximizing the concurrence and the WCE

A direct generalization of Eq. (4a) for  $N$  repeaters yields for the concurrence [27]

$$C^{(N)} = \sum_{\{m_i\}} 2 |\det(X_{\{m_i\}})|, \quad (23)$$

where  $X_{\{m_i\}} = \hat{\varphi} \hat{u}_{m_1} \hat{\varphi} \cdots \hat{u}_{m_N} \hat{\varphi}$ , and the states  $|u_{m_i}\rangle$  are associated with the measurement result  $m_i$  of the  $i$ th repeater. Then the maximization of  $C^{(N)}$  reads

$$\begin{aligned} \max_M \{C^{(N)}\} &= |\det(\hat{\varphi})|^{N+1} \max_M \left\{ \sum_{\{m_i\}} 2^{N+2} \right. \\ &\quad \left. \times |\det(\hat{\Phi} \hat{u}_{m_1} \hat{\Phi} \cdots \hat{u}_{m_N} \hat{\Phi})| \right\} = |2 \det(\hat{\varphi})|^{N+1}, \end{aligned} \quad (24)$$

where  $\hat{\Phi} = 1_2 / \sqrt{2}$  corresponds to a maximally entangled state. For states  $\varphi$  which are not perfect singlets, the concurrence decreases exponentially with  $N$ .

$$C_{\max}^{(N)} \sim (4\varphi_0\varphi_1)^{N/2}, \quad N \gg 1. \quad (25)$$

The same arguments as for the systems of one or two repeaters hold for the WCE, so that XZ Bell measurements

TABLE II. Asymptotic behavior of the SCP for a 1D chain of  $N \gg 1$  repeaters. Three specific measurement protocols are studied: conversion of all states into singlets (CS), XZ and ZZ measurements.

	CS	XZ	ZZ
$S^{(N)}$	$(2\varphi_1)^N$	$< (4\varphi_0\varphi_1)^N$	$< \frac{1}{\sqrt{N}} (4\varphi_0\varphi_1)^{N/2}$

have to be performed on each repeater in order to maximize it.

#### 2. Maximizing the SCP

A similar formula as Eq. (23) for the average SCP is

$$S^{(N)} = \sum_{\{m_i\}} 2 \min\{\text{eig}(X_{m_i} X_{m_i}^\dagger)\}. \quad (26)$$

Contrary to the maximization of the concurrence, we cannot find here such an easy way to calculate the maximum value of  $S$ , but we can already say a few words about the SCP for a 1D chain with a large number of repeaters:

(a) Since  $S$  is always smaller than or equal to  $C$ , it is upper bounded by

$$S_{\max}^{(N)} \lesssim (4\varphi_0\varphi_1)^{N/2}. \quad (27)$$

(b) After  $N \gg 1$  measurements, the entanglement of the resulting states is expected to be, in average, very small, so that the SCP and the concurrence could be related by  $S \approx C^2$ . Hence we may have the asymptotic behavior  $S^{(N)} \sim (4\varphi_0\varphi_1)^N$ .

Even if we do not have the protocol that maximizes the SCP, we present here three specific strategies, as the results are instructive. The first and simplest one consists of trying to convert each state into a singlet, and then to establish a perfect connection between the end qubits of the chain. In the second strategy we perform XZ measurements at all stations, and from Sec. III A 2 we know that all resulting states have the same amount of entanglement. We indeed find the exponential decay of the SCP related to the one of the concurrence. Finally, in Appendix D, we derive the explicit formula for ZZ measurements on a chain of any number of repeaters, which yields a decay of the SCP which is quite close to the upper bound given in Eq. (27). The asymptotic behaviors are summarized in Table II.

### IV. SIMPLEST 2D NETWORK: A SQUARE

The previous section contains our main results for 1D networks. In the remainder of this work, we analyze lattices of dimension larger than one. We study in this section a square made of four identically entangled states (see Fig. 4). This is clearly one of the simplest possible 2D networks. The operations we perform consist of three steps: a first measurement  $M_1$  yielding some outcome  $\alpha$ , then a measurement  $M_2$  depending on  $\alpha$  and giving another state  $\beta$ , and finally, a distillation of these two states to get a final state  $\psi$ . The goal is of course, to get  $\psi$  as entangled as possible, given the states  $\varphi$ .

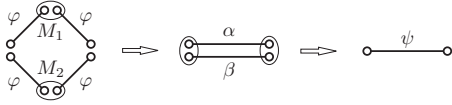


FIG. 4. Operations on a square to obtain an entangled pair on the diagonal: first two measurements, then distillation of the resulting states  $\alpha$  and  $\beta$ .

### 1. Distillation

Majorization theory [22] tells us how entangled the state  $\psi$  can be. Without loss of generality we choose  $\alpha_0 \geq \beta_0$  and the majorization criterion reads

$$(\alpha_0\beta_0, \alpha_0\beta_1, \alpha_1\beta_0, \alpha_1\beta_1) < (\psi_0, \psi_1, 0, 0), \quad (28)$$

whose only nontrivial inequality is  $\alpha_0\beta_0 \leq \psi_0$  (see Appendix B). Since we are looking for a state  $\psi$  that is as entangled as possible, its greatest Schmidt coefficient is

$$\psi_0 = \max \left\{ \frac{1}{2}, \alpha_0\beta_0 \right\}. \quad (29)$$

### 2. Maximizing the figures of merit

Arguments used for 1D networks still hold here, so that one has to perform Bell measurements and XZ measurements to maximize the concurrence and the WCE, respectively. It is worth pointing out that a perfect singlet  $\psi$  can be established with probability one after two XZ measurements followed by optimal entanglement LOCC transformation if  $\varphi$  satisfies

$$\varphi_0 \leq \varphi_0^* = \frac{1 + \sqrt{1 - \sqrt{2(\sqrt{2} - 1)}}}{2} \approx 0.65. \quad (30)$$

Thus we consider that  $\varphi$  is less entangled than  $\varphi^*$  since we already know how to get a singlet for  $\varphi_0 \leq \varphi_0^*$ . We proceed in two steps for maximizing the SCP: we first look at the subproblem of maximization over the measurements  $M_2$  for a given outcome  $\alpha$ , and then we provide some numerical results for the whole square.

*Second measurement.* We first notice that a singlet can be obtained by an XZ measurement with probability one if  $\alpha_0 \leq \alpha_0^* \equiv (1 + \sqrt{1 - (4\varphi_0\varphi_1)^2})^{-1}$ . Then, labeling by  $m$  the resulting states  $\beta$  of the measurement  $M_2$ , we can write the function to be maximized as

$$\begin{aligned} S_M^\Delta &= 2 \sum_m p_m \left( 1 - \max \left\{ \frac{1}{2}, \alpha_0\beta_{m,0} \right\} \right) \\ &= 2\alpha_1 + \alpha_0 2 \sum_m p_m \min \left\{ \beta_{m,1}, \frac{\alpha_0 - \alpha_1}{2\alpha_0} \right\} \\ &\equiv S_{\max}^{(0)}(\alpha_0) + \alpha_0 S_M^{(2)}\left(\varphi_0, \varphi_0, \frac{1}{2\alpha_0}\right), \end{aligned} \quad (31)$$

so that all results of Sec. III B can be applied. The three quantities  $p_{\min}$ ,  $p_{\max}$ , and  $p^*$  used in that section are now  $p_{\min} = \varphi_0\varphi_1$ ,  $p_{\max} = (\varphi_0^2 + \varphi_1^2)/2$ , and  $p^* = \varphi_0\varphi_1\alpha_0/(\alpha_0 - \alpha_1)$ . Since  $p^*$  is greater than  $p_{\min}$  for all states  $\alpha$  and  $\varphi$ , it follows

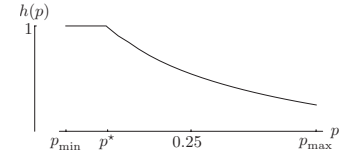


FIG. 5. Typical plot of the function  $h(p)$  governing the SCP of the square.

that  $S_{\max}^\Delta$  is reached by Bell measurements except when  $p^* \in ]p_{\min}, (1 - p_{\max})/3[$ .

*First measurement.* The function to maximize over the measurements  $M_1$  is

$$S_{M_1}^\square = \sum_m p_m S_{\max}^\Delta(\alpha_{m,0}, \varphi_0, \varphi_0). \quad (32)$$

For Bell measurements, since the Schmidt coefficient  $\alpha_{m,0}$  depends on  $p_m$  only, we can write  $S_{M_1}^\square = \sum_m h(p_m)$ . Here we make a slightly abuse of notation, since we again use  $h(p)$ , as in Sec. III B 2. Actually, the shape and properties of the function  $h(p)$  discussed here and in Sec. III B 2 are very similar. Therefore, all arguments used in that section for the maximization of the SCP apply here, too. The plot of  $h(p)$  is shown in Fig. 5. The quantity that corresponds to  $p^*$  is now written  $p^*$  and its value is

$$p^* = \frac{\varphi_0\varphi_1}{2\sqrt{\alpha_0^*\alpha_1^*}},$$

where  $\alpha_1^* \equiv 1 - \alpha_0^*$ . With these definitions, one can check that for all  $\varphi_0$  greater than  $\varphi_0^*$ , we have  $p_{\min} \leq p^*(\varphi_0) \leq 1/4$  and that  $p^* \rightarrow p_{\min}$  when  $\varphi_0 \rightarrow 1$ , whence the best measurements for nearly unentangled states  $\varphi$  are the ZZ ones. As for the system of two repeaters, performing Bell measurements is not the best choice when it is not possible to get three of the four outcome probabilities to be equal to  $p^*$  [but this is possible when  $\varphi_0 \leq \varphi_0^* \approx 0.664$  (see Fig. 6)]. Finally, we summarize the results in Table III, and the similarity with Table I is immediate.

## V. HIERARCHICAL LATTICES

In this section we will directly apply the previous results to study the establishment of entanglement over large scales in lattices with hierarchical geometry. These are lattices that iterate certain geometric structures, so that at each level of iteration the number of nodes or the number of neighbors

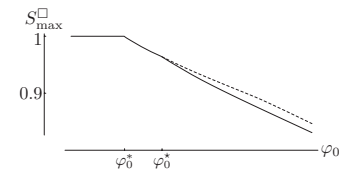


FIG. 6. SCP for a square made of four states  $\varphi$ . Numerical results (dashed line) show that Bell measurements (solid line) do not lead to the optimal solution for  $\varphi_0 > \varphi_0^* \approx 0.664$ .

TABLE III. Maximization of  $S^\square$  over Bell measurements (see the text for details).

Value of $p^*$	$\{p_m\}$ maximizing $S^\square$
$\varphi_0 \rightarrow 1$	$\{p_{\min}, p_{\min}, p_{\max}, p_{\max}\}$
$\varphi_0 \geq \varphi_0^*$	$\{p^*, p^*, p_{\max}, 1 - 2p^* - p_{\max}\}$
$\varphi_0^* \leq \varphi_0 \leq \varphi_0^*$	$\{p^*, p^*, p^*, 1 - 3p^*\}$
$\varphi_0 \leq \varphi_0^*$	$\{1/4, 1/4, 1/4, 1/4\}$

changes. Unfortunately, we do not know how to find optimal strategies for such lattices; we restrict our considerations to show that one can establish perfect entanglement in a finite number of steps at some iteration level. This perfect entanglement can be swapped further to the lowest levels of iteration, i.e., to the largest scales, which can be considered as the largest geometrical distances.

**A. “Diamond” lattice**

We start considering the so-called “diamond” lattice, which is obtained by iterating the operation presented in Fig. 7, in which a single bond (two qubits and one entangled state) is replaced by four bonds forming a diamond shape (four pairs of qubits and four entangled states). We prove that for sufficiently large initial entanglement, one can establish perfect entanglement on large scales (i.e., on some lower levels of iteration) in a finite number of steps.

We assume that the lattice is formed by very many iterations, and that all bonds correspond to entangled states  $|\varphi\rangle = \varphi_0|00\rangle + \varphi_1|11\rangle$ . Our aim is to perform measurements in a recursive way and demonstrate that for sufficiently small  $\varphi_0$  it is possible to establish perfect entanglement on the lowest level of the iteration hierarchy, i.e., between the “parent” nodes  $A$  and  $B$ . In order to keep the form of the network unchanged during the recursive measurement we will apply the WCE strategy to the nodes analogous to  $C$  and  $D$ , starting from the highest (last) iteration level. After applying WCE we obtain with probability 1 a pair of entangled states  $|\psi\rangle = \psi_0|00\rangle + \psi_1|11\rangle$ , with  $\psi_0 = (1 + \sqrt{1 - 16\varphi_0^2\varphi_1^2})/2$ . This pair can then be distilled with probability 1 to a new two-qubit entangled state  $|\varphi'\rangle$  [see Eq. (29)] as follows:

$$\varphi'_0 = \max\left\{\frac{1}{2}, \frac{1}{4}\left(1 + \sqrt{1 - 16\varphi_0^2\varphi_1^2}\right)^2\right\}.$$

Denoting now the SCP by  $E = 2\varphi_1$ , we rewrite the recursion as

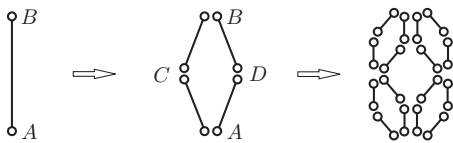


FIG. 7. The diamond lattice is formed by iterating the following operation: a single bond (two qubits and one entangled state) is replaced by four bonds forming a diamond shape (four pairs of qubits and four entangled states). After  $K$  iterations, the nodes  $A, B, C, D$  have  $2^K$  links, the nodes on the next level  $2^{K-1}$  links, etc.

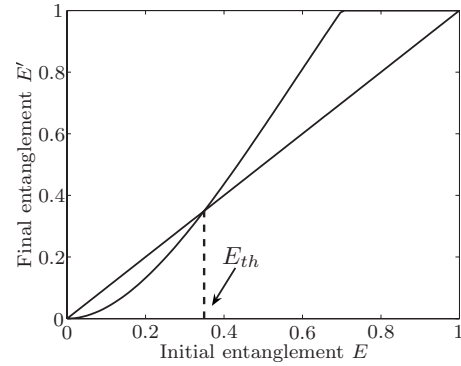


FIG. 8. Recursion relating  $E$  on the higher level of lattice iteration to  $E'$  at the lower level of iteration in the diamond lattice. Each iteration consists of the following steps: (i) WCE and (ii) the two resulting two-qubit states are transformed with probability one into a two-qubit state of the same SCP.

$$E' = 2(1 - \psi_0^2) = 1 + (2 - E)^2 E^2 / 2 - \sqrt{1 - (2 - E)^2 E^2}.$$

This recursion (see Fig. 8) has one nontrivial unstable fixed point  $E_{th}$ , and two trivial stable fixed points  $\tilde{E} = 0$  and  $\tilde{E} = 1$ . The latter is achieved in a finite number of steps provided the initial  $E > E_{th} \approx 0.349$ . Note that  $E_{th}$  is strictly smaller than  $E^* = 2(1 - \varphi_0^*)$  from Eq. (30). For  $E \geq E^*$ ,  $E'$  is equal to 1, i.e., the singlet is achieved in one step.

**B. “Tree” lattice**

Similar results hold for the simplest possible “tree” lattice: a double Cayley tree lattice with a branching factor of two [see Fig. 9(a)]. Let us denote the initial SCP of all bonds by  $E_0$ . The strategy is depicted in Fig. 9(b): the nodes in the middle of the tree perform the WCE. This prepares two two-qubit states between the neighboring nodes with the entanglement, measured by the SCP, equal to  $E_1$ . These two states are then converted with probability 1 into a two-qubit state with  $E = \min\{1, 2[1 - (1 - E_1/2)^2]\}$ , which will undergo recursive transformations [Fig. 9(b)]. We perform then the WCE on one of the three connected bonds, and obtain  $E_1 = 1 - \sqrt{1 - E_0(2 - E_0)E(2 - E)}$ . Then, the WCE is applied to the remaining pair of bonds yielding

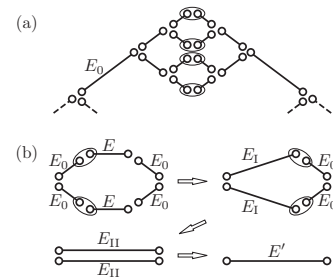


FIG. 9. (a) Tree configuration; (b) The nodes in the middle perform WCE. This creates two two-qubit states between the neighboring nodes. These states are transformed into a two-qubit state of the same SCP. The process is iterated until a perfect singlet is established between the two ends of the tree.

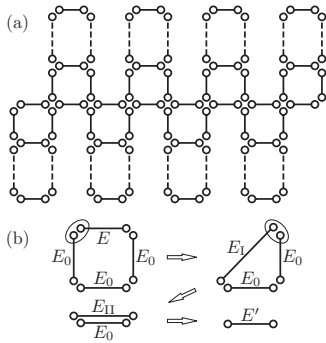


FIG. 10. (a) “Centipede” with its “legs” and “spine.” (b) Recursive measurement scheme; note that the method can be equally well applied also in higher dimensions.

$E_{II} = 1 - \sqrt{1 - E_0(2 - E_0)E_I(2 - E_I)}$ . Finally, the optimal entanglement LOCC conversion is applied to the pair of  $E_{II}$  bonds obtained from the two different but neighboring branches of the tree, yielding, as follows from majorization,  $E' = \min\{1, 2[1 - (1 - E_{II}/2)^2]\}$ . The recursion relations can be rewritten as

$$E' = F(E; E_0). \quad (33)$$

This recursion depends explicitly on  $E_0$ . It is easy to see that since the WCE does not increase the SCP, the recursion (33) will have: (i) only one trivial stable fixed point  $\tilde{E} = 0$  if  $E_0 < E_{th}$ , and (ii) three fixed points otherwise: stable 0, unstable  $\tilde{E}$ , and stable 1 otherwise. Here if we start with  $E \geq E_{th}$  we will end up in one step with  $E' = 1$ . The threshold value is obtained by solving the equation  $1 = 2(1 - \{1 - \sqrt{1 - E_0^2(2 - E_0)^2}/2\}^2)$ , and is given by

$$E_{th} = 1 - \sqrt{1 - \sqrt{2(\sqrt{2} - 1)}} \approx 0.7. \quad (34)$$

## VI. GENUINE 2D LATTICES

In this section we consider genuine 2D lattices when the number of nodes is big. On the one hand, we apply the methods and observations of the previous sections to these large lattices. On the other hand, we reconsider the various variants of the methods employing classical and quantum percolation techniques.

### A. “Centipede” in square lattice

As another example of the power of recursive measurement methods of the previous section, we consider a wide strip of a 2D square lattice and the “centipede” figure within it [see Fig. 10(a)]. Let us denote the initial entanglement as  $E_0$ , and the entanglement at the end bond of a “leg” by  $E$ . We then apply the following measurement scheme to the ends of each of the legs of the centipede (see also Fig. 10): (i) We apply the WCE to  $E_0$  and  $E$ , replacing these two bonds by one with  $E_1 = 1 - \sqrt{1 - E_0(2 - E_0)E(2 - E)}$ ; (ii) we repeat it with the other vertical bond obtaining thus a pair of states at the horizontal end of the leg: one with entanglement  $E_0$  and the

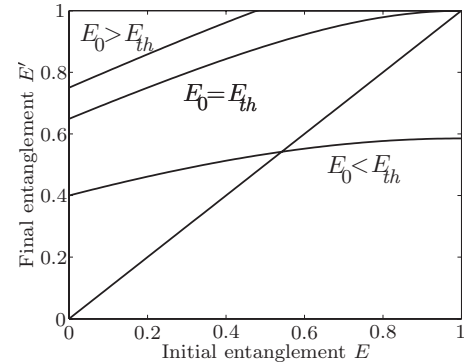


FIG. 11. Recursion relation for the centipede lattice. Only when the entanglement  $E_0$  is larger than a threshold  $E_{th}$ , a trivial stable point at  $E = 1$  appears.

other with  $E_{II} = 1 - \sqrt{1 - E_0(2 - E_0)E_I(2 - E_I)}$ ; (iii) the resulting pair is then distilled with probability 1 to a two-qubit state with  $E' = \min\{1, 2[1 - (1 - E_0/2)(1 - E_{II}/2)]\} = F(E; E_0)$ . This situation is somewhat similar to the case of the tree lattice from the previous section, but not completely. The recurrence relation depends explicitly on  $E_0$  and has always a nontrivial stable fixed point  $\tilde{E} > E_0$ . This fixed point, however, is strictly smaller than 1, when  $E_0$  is small. In the first case, although we do concentrate more entanglement along the “spine” we still have to face the problem that the spine is a 1D network, and will exhibit an exponential decrease of probability of establishing the perfect entanglement for large distances [12]. On the other hand, the stable fixed point is simply  $\tilde{E} = 1$ , provided  $E_0$  is large enough. In this case a perfect singlet is achieved in a finite number of steps, and the singlets from all legs can be concentrated at the spine of the centipede with probability 1. Obviously, all that implies that the width of the strip of the 2D lattice (equal to twice the length of the centipede leg) can be finite: it must be just larger than the number of steps necessary to get a perfect singlet.

The condition for the threshold value of  $E_0$  is easy to derive: we have to put  $E = 1$  in the above recurrence and solve  $1 = 2\{1 - (1 - E_{th}/2)[1 + \sqrt{1 - E_{th}^2(2 - E_{th})^2}/2]\}$ , which gives  $E_{th} \approx 0.649$  (Fig. 11).

### B. Percolation strategies

In Ref. [12] we have pointed out that one possible strategy for entanglement distribution is to convert locally all bonds with probability  $p$  into singlets and then perform entanglement swappings. This strategy can then be linked to classical bond percolation theory, such that all the known results of this field can be applied to our quantum scenario (see also Appendix A): indeed, with probability  $p$  a perfect connection is established between the nodes, otherwise no entanglement between them is left. We name this strategy classical entanglement percolation for obvious reasons. The critical amount of entanglement such that long-distance entanglement distribution is possible simply follows from the comparison of the optimal probability for singlet conversion,

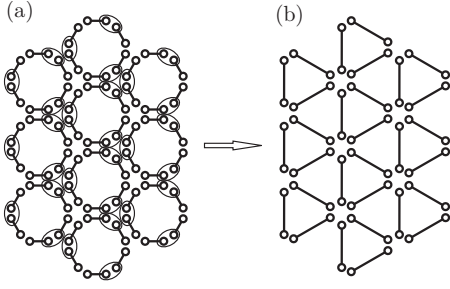


FIG. 12. Each node is connected by two copies of the same two-qubit state  $|\varphi\rangle$ . The nodes marked in (a) perform the measurement optimal according to the SCP. A triangular lattice (b) is obtained where the SCP is the same as for the state  $|\varphi\rangle$ . Classical entanglement percolation is now possible in the new lattice.

resulting from majorization theory, with the classical percolation threshold of the corresponding lattice. That is, whenever this singlet conversion probability is larger than the threshold, long-distance entanglement is possible via classical entanglement percolation. One should stress that classical percolation strategies work for any lattice and dimension. Nevertheless, every percolation strategy relies on the conversion of all bonds to singlets with a certain probability  $p$ , and then a perfect entanglement between two nodes on the large scale is established with a probability  $\theta^2(p)$ . The latter formula expresses the fact that both nodes have to belong to the percolating cluster, which happens for each of them independently with probability  $\theta(p)$  (see Appendix A and [13]). This probability is always smaller than one, except for the trivial case  $p=1$ .

The natural question is whether the thresholds defined by classical percolation theory are optimal or entanglement percolation represents a related but different theoretical problem where new bounds have to be obtained. This is of course equivalent to determining whether the measurement strategy based on local SCP is optimal in the asymptotic regime. Here, we construct several examples that go beyond the classical percolation picture, proving that the classical entanglement percolation strategy is not optimal. The key ingredient for the construction of these examples is the measurement strategy previously obtained for the one-repeater configuration that maximizes the SCP.

### 1. Honeycomb lattice with doubled bonds

The first example (already discussed in Ref. [12]) considers a honeycomb lattice where each node is connected by two copies of the same two-qubit state  $|\varphi\rangle$  [see Fig. 12(a)].

The simplest strategy consists in trying to convert all bonds of the doubled honeycomb lattice into singlets, and then applying entanglement swapping. The percolation threshold of this doubled lattice is not difficult to calculate: at the critical point, the probability that, at each edge, at least one conversion is successful has to be equal to the percolation threshold of the simple honeycomb lattice; if both conversions are successful we simply discard one pair. We thus have  $p_c^\circ = 1 - (1 - 2\varphi_1)^2$ , hence the percolation threshold is (see Table IV)

TABLE IV. Classical (bond) percolation thresholds  $p_c$  for some regular lattices.

Lattice	$p_c$
Triangular	$p_c^\Delta = 2 \sin(\pi/18) \approx 0.347$
Square	$p_c^\square = 0.5$
Honeycomb	$p_c^\circ = 1 - 2 \sin(\pi/18) \approx 0.653$

$$2\varphi_1 = 1 - \sqrt{2 \sin\left(\frac{\pi}{18}\right)} \approx 0.411. \quad (35)$$

We define the classical entanglement percolation strategy as (i) converting in the best possible way *all* bonds shared by two parties into *one* singlet and (ii) applying entanglement swapping to those pairs where a singlet was obtained. If, as above, the Schmidt coefficients of the two-qubit state are  $\varphi_0 \geq \varphi_1$ , the SCP of  $|\varphi\rangle^{\otimes 2}$  is given by  $p_{ok} = 2(1 - \varphi_0^2)$ . We choose this conversion probability to be equal to the percolation threshold for the honeycomb lattice and get

$$2\varphi_1 = 2 \left( 1 - \sqrt{\frac{1}{2} + \sin\left(\frac{\pi}{18}\right)} \right) \approx 0.358. \quad (36)$$

We now show that another strategy yields a better percolation threshold: some of the nodes [see Fig. 12(a)], perform the optimal strategy for the SCP, mapping the honeycomb lattice into a triangular lattice, as shown in Fig. 12(b). What is important is that the SCP for the new bonds is exactly the same as for the initial state  $|\varphi\rangle$ , that is,  $2\varphi_1$ . We choose it to be equal to  $p_c^\Delta$ , so that

$$2\varphi_1 = 2 \sin\left(\frac{\pi}{18}\right) \approx 0.347, \quad (37)$$

which proves that the classical entanglement strategy is not the best one.

### 2. Asymmetric triangular lattice

The second type of examples, although less symmetric, is generic and has a totally different character than the previous one. For simplicity, we show the argument in the case of a triangular lattice, but the same reasoning can be applied to other geometries. Consider the triangular lattice of Fig. 13(a). Solid lines correspond to two-qubit pure states  $|\varphi\rangle$  while dashed lines correspond to states  $|\tilde{\varphi}\rangle$  that are less entangled, i.e.,  $\tilde{\varphi}_0 > \varphi_0$ . We choose the first state such that  $p_{ok} = 2\varphi_1$  satisfies  $p_c^\Delta < p_{ok} < \sqrt{p_c^\Delta}$ . If  $|\tilde{\varphi}\rangle = |\varphi\rangle$ , the classical entanglement percolation strategy works. However, we choose this second less entangled state such that its SCP is small enough to make the classical entanglement percolation impossible. This state always exists. Indeed, note that when  $\varphi_1 \rightarrow 0$ , these states can simply be removed from the lattice, and classical entanglement percolation fails because of  $p_{ok}^2 < p_c^\Delta$ . It is now rather straightforward to construct a successful entanglement percolation strategy: the state  $|\tilde{\varphi}\rangle$  is discarded and the optimal strategy for the one-repeater configuration and the SCP is performed. The lattice is then mapped into a new triangular lattice keeping the conversion probabil-

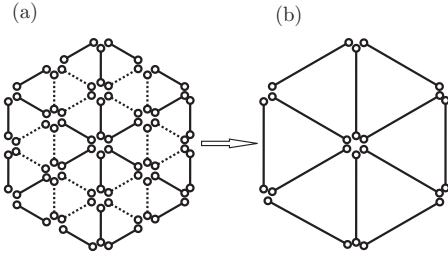


FIG. 13. The triangular lattice consists of two different entangled states  $|\varphi\rangle$  and  $|\bar{\varphi}\rangle$  for the solid and dashed lines, respectively. The less entangled states  $|\bar{\varphi}\rangle$  are discarded and some of the nodes perform the optimal measurement according to the SCP. A new triangular lattice is obtained, governed by the SCP of  $|\varphi\rangle$ .

ity of the first, more entangled state [see Fig. 13(b)]. Classical entanglement percolation can now be applied to this new lattice, since  $p_{ok} > p_c^\Delta$ .

### C. Doubling the square lattice

The final example deals with a square lattice and has yet another character. Here we replace every second pair of horizontal bond by a single one using the optimal SPC strategy, which as we know from Sec. III does not change the SCP on average, replacing, however, pure states by a known mixture. The same is done with every second pair of vertical bonds. In effect we replace the original square lattice by two disjoint lattices with the lattice constant twice bigger than the original one, but the same SCP (see Fig. 14). Now we are interested in establishing entanglement between any of the two neighboring nodes  $A, A'$  and  $B$  or  $B'$ , at large distances.

In the case of doubled lattices the calculation is simple: the pairs  $(A, B)$  and  $(A', B')$  belong to two disjoint lattices, and the probability that, say,  $(A, B)$  belongs to the percolating cluster is equal asymptotically to  $\theta^2(p)$ . The probability that at least one of the pairs belongs to the percolating cluster is thus

$$P_{\text{double}} = 1 - (1 - \theta)^2 = \theta^2(2 - \theta^2). \quad (38)$$

This probability has to be compared with the probability that at least one of the pairs  $(A, B)$ ,  $(A', B)$ ,  $(A, B')$ , or  $(A', B')$  belongs to the percolating cluster in the original square lat-

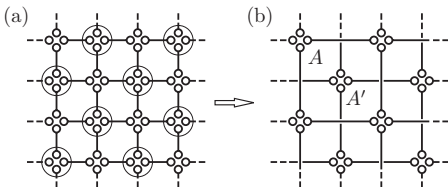


FIG. 14. (a) Measurements necessary to double the square lattice: the marked nodes apply the optimal one-repeater transformation along the vertical and horizontal directions. (b) Resulting pairs of disjoint square lattices with lattice constant doubled; we want to establish perfect entanglement between any two neighboring points  $A, A'$  versus  $B$  and  $B'$ .  $A$  and  $A'$  ( $B$  and  $B'$ ) are neighbors but belong to different lattices.

tice. The latter probability is asymptotically  $\pi^2$ , where  $\pi$  is the probability that  $A$  or  $A'$  (or equivalently  $B$  or  $B'$ ) belongs to the percolating cluster  $\mathcal{C}$ . Thus we have

$$\pi = P[A \text{ or } A' \in \mathcal{C}] = P[A \in \mathcal{C}] + P[A' \in \mathcal{C}] - P[A, A' \in \mathcal{C}].$$

In order to estimate the last term in the above expression, we use the celebrated Fortuin-Kasteleyn-Ginibre (FKG) inequality ([28], see also [13]). To state it, we first define an event described in terms of a percolation configuration to be *increasing* if it has the property that, once it holds for a certain bond configuration, it holds for all configurations obtained by adding bonds to the initial one. FKG inequality says that any two such events are positively correlated. The events  $\{A \in \mathcal{C}\}$  and  $\{A \leftrightarrow A'\}$  (“ $A$  and  $A'$  are connected by a path of maximally entangled bonds”) are clearly increasing and, since their intersection is the event  $\{A, A' \in \mathcal{C}\}$ , it follows that

$$P[A, A' \in \mathcal{C}] \geq P[A \in \mathcal{C}]P[A \leftrightarrow A']. \quad (39)$$

Denoting  $P[A \leftrightarrow A']$  by  $\tau$ , we thus have  $\pi^2 \leq \theta^2(2 - \tau)^2$ . Therefore, doubling the square lattice is a better strategy than the classical percolation, i.e.,  $\pi^2 \leq P_{\text{double}}$ , whenever

$$(2 - \tau)^2 \leq 2 - \theta^2. \quad (40)$$

We believe that this inequality is fulfilled for all  $p$ , but we have not been able to prove it. Below we present a computer assisted proof that it holds when  $p$  is just above the percolation threshold  $p_c^\square = 0.5$ , i.e., when  $\theta$  tends to zero. Setting  $\theta = 0$  in the inequality (40), we immediately see that proving Eq. (40) in this limit requires one to demonstrate that  $2 - \tau \leq \sqrt{2}$ . We may try to estimate  $\tau$  from below by considering the six shortest trajectories connecting  $A$  and  $A'$ : the most direct, two two-bond paths, and the two pairs of four-bond paths around the adjacent squares. One finds

$$\tau > 2(p^2 + 2p^4 - 2p^5) - (p^2 + 2p^4 - 2p^5)^2.$$

Unfortunately, for  $p = p_c^\square = 1/2$  this estimate is too small and thus not sufficient to prove Eq. (40), since it gives only  $2 - \tau < 1.473 \dots$ . One can improve the estimate analytically by adding further paths connecting  $A$  and  $A'$ ; this procedure becomes, however, technically tedious. We have therefore turned to the standard numerical Monte Carlo method of calculating the transition probability from  $A$  to  $A'$ . The method we used generates the shortest paths (like the ones used for calculating the above estimate) automatically, while the longer ones are generated using the Monte Carlo sampling. For  $p > p_c^\square$  the convergence is exponential: if we plot a subsequent estimate of  $\tau$  as a function of the maximum cluster size allowed in the Monte Carlo sampling, it approaches the final value exponentially fast for large clusters. As expected, the convergence is algebraic at  $p = p_c^\square$ : the estimate of  $\tau$  approaches its final value as a power of the cluster size. A power law fit and a comparison with the values just above the percolation threshold give with a very good accuracy  $\tau \approx 0.687$  and hence  $2 - \tau \approx 1.313 < \sqrt{2}$ . Q.E.D.

This is yet another result which does not have a classical analog, showing how quantum mechanical measurements can improve the classical percolation strategy.

## VII. CONCLUSION

In this paper, we have considered the problem of entanglement percolation through pure-state quantum networks. We have first focused our investigations on small quantum networks. Even for these particularly simple systems, interesting and unexpected properties have been pointed out. One of the main results is the description of a Bell measurement by its outcome probabilities only (Result 1). This has allowed us to maximize the different figures of merit introduced at the beginning of the paper. We have shown, then, that Bell measurements do not yield in general the optimal protocol, even for a chain consisting of only two repeaters.

The results for small lattices have later been used as building blocks for entanglement percolation protocols in asymptotically large lattices. We have provided several examples illustrating some of the properties characterizing these lattices: recursive relations, classical entanglement percolation, and examples of lattices where quantum effects allow one to go beyond classical percolation.

In general, little is still known about the problem of entanglement percolation, that is, the distribution of entanglement through quantum networks. In the pure-state case, it would be interesting to derive lower bounds to the amount of entanglement between the nodes such that entanglement percolation is possible. The main question, however, is to extend these results to the mixed-state scenario, providing examples of entanglement percolation protocols for lattice with mixed-state bonds.

## ACKNOWLEDGMENTS

We thank John Lapeyre who kindly supplied us with a high-precision numerical value of  $P[A \leftrightarrow A']$  in Sec. VI C. Much of this work was supported by the QCCC program, part of the Elite Network of Bavaria (ENB). We also acknowledge support from the cluster of excellence Munich Centre for Advanced Photonics (MAP), the Deutsche Forschungsgemeinschaft, the EU IP programs “SCALA” and “QAP;” the European Science Foundation PESC QUDEDIS, and the MEC (Spanish Government) under Contracts No. FIS 2005-04627, No. FIS 2004-05639, and Consolider QOIT. J.W. acknowledges NSF Grant No. DMS-0623941.

## APPENDIX A: CLASSICAL PERCOLATION

Classical percolation is perhaps one of the most fundamental examples of critical phenomenon, since it is a purely statistical one [13]. At the same time it is one of the most universal ones, since it describes a whole variety of physical, biological, or ecological processes [14]. In bond percolation we consider typically a regular lattice of nodes connected by random bonds, the probability of having a bond between two neighboring nodes being  $p$ . For an infinite lattice of a given dimension, one would like to know whether an infinite open cluster exists, that is, whether there is a path of connected points of infinite length through the lattice. It turns out that this infinite cluster appears if, and only if, the probability of connection  $p$  is larger than a critical threshold  $p_c$ , which

depends on the lattice. The values of  $p_c$  for some commonly used lattices are given in Table IV.

A quantity of primary interest very related to the percolation threshold is the *percolation probability*  $\theta(p)$ , being the probability that a given node belongs to an infinite open cluster. Clearly,  $\theta(p)=0$  for  $p < p_c$ , while  $\theta(p) > 0$  for  $p > p_c$ . Another quantity of direct interest for us is the two-point connectivity function  $\tau(x, y)$ , which gives the probability that  $x, y$  belong to the same open cluster of bonds. Above  $p_c$ , this probability is  $\theta^2(p)$ ; below it decays exponentially; for instance, for a hypercubic lattice in  $d$  dimensions, it behaves as  $\tau(0, x) \leq [1 - \xi(p)]^{|x|}$ , where  $\xi(p)$  is the mean cluster size (which is finite below  $p_c$ ), and  $|x|$  is the number of edges (bonds) in the shortest path from 0 to  $x$ .

Connectivity functions concern probabilities in an infinite network. For us it is more natural to assume a finite size network, and paths that join the input and output ports and lie within the finite network. This is related to the so-called *crossing probabilities*, which have been intensively studied in the last years in 2D, using conformal invariance at criticality (for a review, see [29]). Here, a lot of exact results are known; for example, the celebrated Cardy [30] formula says that the crossing probability in the triangular lattice from a vortex of an equilateral triangle to a part of its opposite edge of relative length  $a$ , is simply  $a$ . Generalization of this result to other geometries using conformal invariance is known as Cardy-Carleson law.

## APPENDIX B: LOCC TRANSFORMATIONS AND MAJORIZATION THEORY

Consider two pure states  $|\psi_1\rangle$  and  $|\psi_2\rangle$  in a bipartite system. Can  $|\psi_1\rangle$  be transformed into  $|\psi_2\rangle$  by LOCC in a deterministic way? The solution to this question was obtained in 1999 by Nielsen, who noticed a connection between this problem and majorization theory. Based on this connection, Vidal extended Nielsen’s results, obtaining the optimal probability for LOCC conversion between states whenever a deterministic transformation is impossible [21]. In this Appendix, we review the main results on the connection between majorization theory and LOCC transformations between bipartite pure states (for more details, see [22]). This formalism is extensively employed in many of the LOCC protocols described in this work.

Let us start by introducing the concept of majorization. Consider two  $d$ -dimensional real vectors,  $\vec{v}=(v_0, \dots, v_{d-1})$  and  $\vec{w}=(w_0, \dots, w_{d-1})$ , whose components are positive and sum up to one, and where the components of both vectors are sorted in decreasing order. Then  $\vec{v}$  is said to be majorized by  $\vec{w}$ , denoted by  $\vec{v} < \vec{w}$ , whenever

$$v_0 \leq w_0$$

$$v_0 + v_1 \leq w_0 + w_1$$

$$\vdots$$

$$v_0 + \dots + v_{d-2} \leq w_2 + \dots + w_{d-2}, \quad (\text{B1})$$

while, of course,  $\sum_i v_i = \sum_i w_i = 1$  because of the normalization. Supermajorization is a related notion that is also relevant in our context. Consider the same vectors as above but now with components in increasing order. We denote these components by  $v_i^\uparrow$  and  $w_i^\uparrow$ , where  $v_i^\uparrow = v_{d-i-1}$  and similarly for  $w$ . The vector  $\vec{v}$  is now submajorized by  $\vec{w}$ , denoted by  $\vec{v} <^w \vec{w}$  when

$$\sum_{i=0}^k v_i^\uparrow \geq \sum_{i=0}^k w_i^\uparrow, \quad (\text{B2})$$

for all  $k=0, \dots, d-1$ . Here, we do not impose any normalization on the vectors.

Coming back to our initial question on the LOCC transformation between pure states,  $|\psi_1\rangle$  can be transformed into  $|\psi_2\rangle$  with probability one whenever  $\vec{\alpha}^{\psi_1} < \vec{\alpha}^{\psi_2}$ , where  $\vec{\alpha}^{\psi_i}$  is the vector of Schmidt coefficients of the state  $|\psi_i\rangle$ . Moving now to probabilistic transformations, the optimal probability for LOCC conversion between the two states is given by the maximum value of  $p$  such that  $\vec{\alpha}^{\psi_1} <^w p \vec{\alpha}^{\psi_2}$ . We refer the interested reader to the original references for details.

As an application of this formalism, and because of its importance in relation to this work, consider the transformation of a state  $|\psi\rangle \in \mathbb{C}^d \otimes \mathbb{C}^d$  of Schmidt coefficients  $\vec{\alpha}^\psi = (\alpha_0, \dots, \alpha_{d-1})$ , in decreasing order, into a singlet. Then, the optimal probability of transformation reads

$$p = \min\{2(1 - \alpha_0), 1\}, \quad (\text{B3})$$

which easily follows from Eq. (B2).

### APPENDIX C: PROOF OF RESULT 1

We prove here that there always exists a Bell measurement which yields outcome probabilities  $p_m$  equal to  $x_m$ , when these values add up to one and lie in the interval  $[p_{\min}, p_{\max}]$ .

*Proof (by contradiction).* Let us write  $\{\mu_m\}$  the four states of the Bell measurement in the magic basis. Because the matrix  $(\mu_{m,i})$  is orthogonal, the conditions on  $x$  are clearly necessary. In fact, we know from Eq. (8) that  $p_m = p_{\min} k_m + p_{\max}(1 - k_m)$  with  $k_m \in [0, 1]$ . One of the four equations of the system  $\{p_m\} = \{x_m\}$  will be dependent on the other three: if we can find three orthogonal vectors  $\mu_m$  such that  $p_m = x_m$  for, say,  $m=1, 2, 3$ , then the fourth one is fixed (up to a sign) with, obviously,  $p_4 = x_4$ . Let us write these three states  $\mu_m$  as

$$\mu_m = (\sqrt{k_m} \cos(\theta_m), \sqrt{k_m} \sin(\theta_m),$$

$$\sqrt{1 - k_m} \cos(\omega_m), \sqrt{1 - k_m} \sin(\omega_m),$$

where  $k_m = (p_{\max} - x_m) / (p_{\max} - p_{\min})$ . By construction, these vectors are normalized and satisfy  $p_m = x_m$ . We now have to prove that there always exist some angles  $\theta_m$  and  $\omega_m$  such that these three vectors are orthogonal. Without loss of generality we order the  $k$ 's such that  $1 \geq k_1 \geq k_2 \geq k_3 \geq k_4 \geq 0$ . Since the probabilities add up to 1 and that  $p_{\min} + p_{\max} = 0.5$  we have

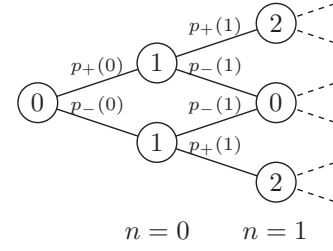


FIG. 15. “Tree view” of the labels  $m$  and their corresponding probabilities after the first two measurements. For symmetry, we choose the root of this tree corresponding to  $n=-1$ .

$$k_1 + k_2 + k_3 + k_4 = 2. \quad (\text{C1})$$

Introducing the notations  $k'_m \equiv 1 - k_m$ ,  $\theta_a \equiv \theta_1 - \theta_2$ ,  $\theta_b \equiv \theta_1 - \theta_3$ ,  $\omega_a \equiv \omega_1 - \omega_2$ ,  $\omega_b \equiv \omega_1 - \omega_3$  and using the identity  $\cos(x)\cos(y) + \sin(x)\sin(y) = \cos(x-y)$ , the conditions of orthogonality read

$$0 = \sqrt{k_1 k_2} \cos(\theta_a) + \sqrt{k'_1 k'_2} \cos(\omega_a),$$

$$0 = \sqrt{k_1 k_3} \cos(\theta_b) + \sqrt{k'_1 k'_3} \cos(\omega_b),$$

$$0 = \sqrt{k_2 k_3} \cos(\theta_a - \theta_b) + \sqrt{k'_2 k'_3} \cos(\omega_a - \omega_b). \quad (\text{C2})$$

The cases  $k_m=0$  or  $k_m=1$  for some  $m$  can be trivially solved, so we consider  $k_m \neq 0$  and  $k'_m \neq 0$ . We have four parameters  $\theta_{a,b}$  and  $\omega_{a,b}$  which can be freely chosen in the interval  $[0, \pi]$ , but the two inequalities  $\sqrt{k_1 k_2} \geq \sqrt{k'_1 k'_2}$  and  $\sqrt{k_1 k_3} \geq \sqrt{k'_1 k'_3}$  impose the constraints  $\theta_a \in [\theta_a^*, \pi - \theta_a^*]$  and  $\theta_b \in [\theta_b^*, \pi - \theta_b^*]$ , with  $\theta_{a,b}^* \in [0, \frac{\pi}{2}]$  such that  $\sqrt{k_1 k_2} \cos(\theta_a^*) = \sqrt{k'_1 k'_2}$  and  $\sqrt{k_1 k_3} \cos(\theta_b^*) = \sqrt{k'_1 k'_3}$ . Thus  $\cos(\omega_a - \omega_b) \in [-1, 1]$  and  $\cos(\theta_a - \theta_b) \in [-\cos(\theta_a^* + \theta_b^*), 1]$ . Then, one can verify that there always exists at least one solution of Eq. (C2), except when  $-\sqrt{k_2 k_3} \cos(\theta_a^* + \theta_b^*) > \sqrt{k'_2 k'_3}$ , which never happens. In fact, suppose that this last inequality holds and rewrite it in terms of  $k_1, k_2$ , and  $k_3$  only. After some tedious algebra and using some trigonometric identities, one finds that the inequality  $k_1 + k_2 + k_3 > 2$  holds, but this is in contradiction with Eq. (C1), which concludes the proof. ■

### APPENDIX D: SCP OF ZZ MEASUREMENTS ON A 1D CHAIN

Even if the number of outcomes grows exponentially with the number of repeaters, one can keep track of all of them in an efficient way. In fact, after any number  $n \leq N$  of entanglement swappings in the ZZ basis, any possible resulting state has the form (up to local unitaries)

$$|m\rangle \equiv \frac{1}{\sqrt{\varphi_0^m + \varphi_1^m}} (\sqrt{\varphi_0^m} |00\rangle + \sqrt{\varphi_1^m} |11\rangle), \quad m \in \mathbb{N}.$$

We prove this by induction on  $n$ , the case  $n=0$  corresponding to the initial state  $m=1$ . Suppose that the result holds and that we got the state  $|m\rangle$  after  $n < N$  measurements. It is easy

to show from Eq. (18) that an entanglement swapping in the ZZ basis on  $|m\rangle \otimes |\varphi\rangle$  is described by

$$|m\rangle \mapsto \begin{cases} |m+1\rangle & \text{with probability } p_+(m) \\ |m-1\rangle & \text{with probability } p_-(m), \end{cases} \quad (\text{D1})$$

where  $p_+(m) = (\varphi_0^{m+1} + \varphi_1^{m+1}) / (\varphi_0^m + \varphi_1^m)$  and  $p_-(m) = 1 - p_+(m)$ , Q.E.D.

The first step to calculate the SCP of this protocol is to compute its variation after a ZZ measurement. Considering that the set  $\{(p_i, |m_i\rangle), i=1, \dots, l\}$  describes all the resulting states of  $n$  measurements, and writing  $\lambda_{\pm}(m)$  the smallest Schmidt coefficient of  $|m \pm 1\rangle$ , the new SCP reads

$$\begin{aligned} S_{ZZ}^{(n+1)} &= \sum_{i=1}^l p_i 2[p_+(m_i)\lambda_+(m_i) + p_-(m_i)\lambda_-(m_i)] \\ &= S_{ZZ}^{(n)} - (\varphi_0 - \varphi_1)p(m=0, n), \end{aligned} \quad (\text{D2})$$

where  $p(m=0, n)$  stands for the probability of getting the

state  $|m=0\rangle$  after  $n$  measurements. Since this probability is not zero for  $n$  odd only, it results that the SCP decreases for  $n$  even only. We have now to calculate the probability  $p(m=0, n)$  of getting a singlet after  $n$  measurements: it is the weighted sum over all possible paths  $\Gamma$  that go from the root node  $m=0$  to the node  $m=0$  at position  $n$  in the tree drawn in Fig. 15. We notice that the weight  $w$  depends on  $n$  only and not on  $\Gamma$ . This is indeed the fact since  $p_+(m)p_-(m+1) = \varphi_0\varphi_1$  for all  $m$  and because we have to go up in the tree as many times as we have to go down. Thus, for  $n$  odd we have  $w(n) = (\varphi_0\varphi_1)^{(n+1)/2}$  and using basic combinatorial analysis one finds that  $p(m=0, n) = (\varphi_0\varphi_1)^k \binom{2k}{k}$ , with  $k = \frac{1}{2}(n+1) \in \mathbb{N}$ . Finally, denoting by  $[x]$  the integer part of  $x$ , the general expression of the SCP for a chain of  $N$  repeaters reads

$$S_{ZZ}^{(N)} = 1 - (\varphi_0 - \varphi_1) \sum_{k=0}^{[N/2]} (\varphi_0\varphi_1)^k \binom{2k}{k}. \quad (\text{D3})$$

- 
- [1] J. I. Cirac, P. Zoller, H. J. Kimble, and H. Mabuchi, *Phys. Rev. Lett.* **78**, 3221 (1997).
- [2] A. D. Boozer, A. Boca, R. Miller, T. E. Northup, and H. J. Kimble, *Phys. Rev. Lett.* **98**, 193601 (2007).
- [3] A. K. Ekert, *Phys. Rev. Lett.* **67**, 661 (1991).
- [4] C. H. Bennett, G. Brassard, C. Crepeau, R. Jozsa, A. Peres, and W. K. Wootters, *Phys. Rev. Lett.* **70**, 1895 (1993).
- [5] J. I. Cirac, A. K. Ekert, S. F. Huelga, and C. Macchiavello, *Phys. Rev. A* **59**, 4249 (1999).
- [6] H.-J. Briegel, W. Dür, J. I. Cirac, and P. Zoller, *Phys. Rev. Lett.* **81**, 5932 (1998).
- [7] W. Dür, H.-J. Briegel, J. I. Cirac, and P. Zoller, *Phys. Rev. A* **59**, 169 (1999).
- [8] L. I. Childress, J. M. Taylor, A. Sørensen, and M. D. Lukin, *Phys. Rev. A* **72**, 052330 (2005).
- [9] L. Hartmann, B. Kraus, H.-J. Briegel, and W. Dür, *Phys. Rev. A* **75**, 032310 (2007).
- [10] M. Zukowski, A. Zeilinger, M. A. Horne, and A. K. Ekert, *Phys. Rev. Lett.* **71**, 4287 (1993).
- [11] See, for instance, *Nature (London)* **432**, 482 (2004); C. A. Muschik, K. Hammerer, E. S. Polzik, and J. I. Cirac, *Phys. Rev. A* **73**, 062329 (2006); A. V. Gorshkov, A. Andre, M. D. Lukin, and A. S. Sorensen, *ibid.* **76**, 033804 (2007); and eprint arXiv:0704.1737.
- [12] A. Acín, J. I. Cirac, and M. Lewenstein, *Nat. Phys.* **3**, 256 (2007).
- [13] G. Grimmett, *Percolation* (Springer-Verlag, Berlin, 1999).
- [14] D. Stauffer, *Introduction to Percolation Theory* (Taylor and Francis, London, 1985).
- [15] M. Keller, B. Lange, K. Hayasaka, W. Lange, and H. Walther, *Nat. Phys.* **431**, 1075 (2004).
- [16] M. D. Eisaman, A. André, F. Massou, M. Fleischhauer, A. S. Zibrov, and M. D. Lukin, *Nat. Phys.* **438**, 837 (2005).
- [17] S. Bose, V. Vedral, and P. L. Knight, *Phys. Rev. A* **60**, 194 (1999).
- [18] J. Modławska and A. Grudka, arXiv:quant-ph/0708.0667.
- [19] E. Knill, R. Laflamme, and G. J. Milburn, *Nature (London)* **409**, 46 (2001).
- [20] S. Hill and W. K. Wootters, *Phys. Rev. Lett.* **78**, 5022 (1997).
- [21] G. Vidal, *Phys. Rev. Lett.* **83**, 1046 (1999).
- [22] M. A. Nielsen and G. Vidal, *Quantum Inf. Comput.* **1**, 76 (2001).
- [23] C. H. Bennett, H. J. Bernstein, S. Popescu, and B. Schumacher, *Phys. Rev. A* **53**, 2046 (1996).
- [24] M. A. Nielsen, *Phys. Rev. Lett.* **83**, 436 (1999).
- [25] S. Bose, V. Vedral, and P. L. Knight, *Phys. Rev. A* **57**, 822 (1998).
- [26] L. Hardy and D. D. Song, *Phys. Rev. A* **62**, 052315 (2000).
- [27] F. Verstraete, M. A. Martín-Delgado, and J. I. Cirac, *Phys. Rev. Lett.* **92**, 087201 (2004).
- [28] C. M. Fortuin, P. W. Kasteleyn, and J. Ginibre, *Commun. Math. Phys.* **22**, 89 (1971).
- [29] S. Smirnov, *C. R. Acad. Sci., Ser. I: Math.* **333**, 239 (2001).
- [30] J. Cardy, *J. Phys. A* **25**, L201 (1992).